

Study of Transport Properties of Mineral Chalcopyrite (CuFeS_2) at Relatively Low Temperatures (77-300 K)

Shabana Rizvi^a, Syed Munir Mehdi Raza Naqvi^a, Syed Mohsin Raza^b,
Syed Dabir Hasan Rizvi^{**} and Shaikh Kamaluddin^c

^aDepartment of Physics, University of Karachi, Karachi - 75270, Pakistan

^bDepartment of Physics, University of Balochistan, Quetta, Pakistan

^cPCSIR Laboratories Complex, Shahrah-e-Dr. Salimuzzaman Siddiqui, Karachi - 75280, Pakistan

(received February 20, 2010; revised April 9, 2010; accepted April 12, 2010)

Abstract. The electrical resistivity and thermoelectric power measurements were carried out on chalcopyrite; the mineral rock sample of Balochistan, Pakistan, in a temperature range down from liquid nitrogen temperature up to room temperature (77-300 K). The resistivity studies show diverse transitions at different temperature intervals especially a semi-superconductivity, where weak fermions (not the Cooper pairs) are produced. This transition is accompanied with another relatively low temperature transition, i.e., a metal-insulator transition which sets in at 92 K. The metal to insulator transition at 92 K occurs due to breakup of weak fermions. The Grüneisen function shows a transition at 215 K, where some kind of phonons become free from their respective Brillouin zones. Thus chalcopyrite at 215 K can produce excited phonons for semiconductor, imaging, nanotube, quantum well, optoelectronic and other devices. The sudden escalation of positive thermoelectric power at 240 K in chalcopyrite shows a phase transition perhaps due to diffusional recovery processes, i.e., shuffling of electrons and positive ion cores. Thermoelectric power measured shows an increasing trend similar to that of the theoretically estimated values with a room temperature value around 600 $\mu\text{V/K}$.

Keywords: transport mechanism, mineral ore, chalcopyrite, electrical resistivity, thermoelectric power.

Introduction

The electrical resistivity of liquid quenched amorphous alloys has been previously studied (Naqvi *et al.*, 1995a; 1995b; Raza *et al.*, 1995) in which methods for estimation of Debye temperature, Debye wave vector, Debye velocity, Fermi wave vector, Fermi velocity, Fermi energy, relaxation time, mean free path, temperature coefficient and activation energy were presented. Use of Arrhenius plot for calculations of activation energy has indicated some thermally activated processes in metallic glasses, which would decipher the temperature dependent activation energies accompanying multiple transitions (Naqvi *et al.*, 1991). Metal-insulator transition in iron-zirconium alloys were observed at relatively high temperatures (Naqvi *et al.*, 1997).

Our previous studies tuned us to study the rock minerals, pyrite (FeS_2) (Naqvi *et al.*, 2007) and chalcopyrite (CuFeS_2). Earlier, we had analyzed the ore samples of Balochistan, Pakistan by X-ray diffraction (XRD); magnetic properties of pyrite (FeS_2) and chalcopyrite (CuFeS_2) from these ore samples were also studied in the temperature range of 77-300 K, showing an overall paramagnetic nature of both pyrite and chalcopyrite (Naqvi *et al.*, 2005). The electron density distributions of pyrite (FeS_2) and chalcopyrite (CuFeS_2) have been recently studied by Gibbs *et al.* (2007).

*Author for correspondence; E-mail: ictpdabir@gmail.com

Apart from being a major ore of copper, chalcopyrite has several other interesting properties. Kametani (1982a), gave a method for thermoelectric power measurement of pulverized metal sulphide ores, including chalcopyrite. Thermoelectric power of pulverized samples of chalcopyrite from various mines was measured (Kametani, 1982b), indicating its *n*-type semiconducting character; the ionization energy obtained was 0.1-0.3 eV. In another study Kametani and Kobayashi (1990) measured the thermoelectric power for particulate chalcopyrite samples from Mount Isa mine. The thermal expansion of synthetic CuFeS_2 was studied at 4-300 K by Sirota *et al.* (1989a); at 5-300 K, the coefficients were negative; the Grüneisen coefficient was also determined. Sirota *et al.* (1991; 1989b) also studied lattice dynamics of chalcopyrite in this low temperature range by X-ray diffractometry, determining the Debye-Waller temperature factor and mean square atomic displacements for the ions. Nkoma and Ekosse (1999) applied X-ray diffraction technique to the ore samples and obtained the lattice parameters for chalcopyrite. The phonon and magnon dispersion of chalcopyrite has been reported by Harris *et al.* (1997). Its electronic structure has been studied by Kurmaev *et al.* (1998) and Fujisawa *et al.* (1994). Donovan and Reichenbaum (1958) compared the electrical properties of synthetic and natural chalcopyrite. Teranishi (1962; 1961) studying the magnetic and electrical properties of chalcopyrite found that it had low electrical conductivity.

In a recent study, these properties in the temperature range of 77-300 K were studied by Khabibullin *et al.* (2009) along with NMR spectrum. They found different low temperature conductivity behaviour for different samples. Semiconductors of chalcopyrite have several applications, such as in photo voltaic devices, solar batteries, non-linear optical devices and luminescence diodes (Shay and Wernick, 1975). Chalcopyrite has its applications in most modern devices ranging from imaging devices, quantum nanodevices and optoelectronic devices (Steiner *et al.*, 2009; Ishii *et al.*, 2008; Kohara *et al.*, 2005; Vincent *et al.*, 2005; Lee *et al.*, 2003; Bai *et al.*, 2002).

In the present work, measurements of thermoelectric power and electrical resistivity of chalcopyrite (CuFeS_2), in the temperature range, 77-300 K have been carried out. Grüneisen function (Barnard, 1972; Rosenberg, 1963) and various other parameters have also been calculated (Table 1 and 2) using the technique employed in our previous work on chalcopyrite (CuFeS_2) (Naqvi *et al.*, 1997; Raza *et al.*, 1995; Barnard, 1972).

Materials and Methods

The rock samples of chalcopyrite were cut in the shape of parallelepiped of size $2 \times 6 \times 10$ mm. The standard four probe method was employed for the electrical resistivity measurement on polished samples of chalcopyrite. A constant current source, Digistant-6426 and Keithley multimeter, 175 & 197A were used in the low temperature measurement of electrical resistivity. Thermoelectric power measurements were carried out using the differential method, as described elsewhere (Naqvi *et al.*, 1993).

Results and Discussion

Electrical resistivity *vs* temperature plot of chalcopyrite is shown in Fig. 1. Fig. 2, represents the Arrhenius plot ($\log \rho$ *vs* $\frac{1000}{T}$) for electrical resistivity of chalcopyrite. Fig. 3 and 4 show Grüneisen function *vs* temperature and thermoelectric power *vs* temperature curves, respectively, for chalcopyrite, in the range, 77-300 K. With Arrhenius plot, the transition regions can be studied on the basis of theory of Raza *et al.* (1995). The labelled transition regions of electrical resistivity at various temperatures are shown in Fig. 1. AB-transition shows metallic behaviour, BB'- semi-metallic, where the conduction electrons are trapped, B'C- metal softening, where the deep energy levels are becoming shallow, CD-semi-conductivity, where the onset of semi-conductivity at 208 K is observed and DE- semi-superconductivity, where weak fermions are produced (not the Cooper pairs). With lowering of temperature from 120 K to 80 K, transition-EF was observed which shows a sudden increase in electrical resistivity thereby indicating that the weak fermions are

broken at low temperatures, i.e., at about 92 K. EF is ascribed to a metal-insulator transition. This is evident by mean free path of 102.24 m at 92 K (at E; end of DE region). These transitions can be ascertained with the help of Arrhenius plot as shown in Fig. 2.

The Bloch-Grüneisen function, \mathcal{G} (Barnard, 1972; Rosenberg, 1963) was calculated using:

$$\mathcal{G} = \text{constant} \times \frac{T^5}{M\theta^6} \int_0^{\theta/T} \frac{z^5 dz}{(e^z - 1)(1 - e^{-z})} \quad (1)$$

where:

T = temperature in Kelvin,

θ = Debye temperature,

z = atomic number,

M = atomic weight and

constant = characteristic of the metal.

A spherical fermi-surface was assumed, neglecting the Umklapp processes. Thus, a Debye-type lattice spectrum is being dealt with. At high temperatures, ($T > \frac{\theta}{2}$), equation (1) get reduced to:

$$\mathcal{G} = \text{constant} \times \frac{T}{4M\theta^2} \quad (2)$$

and at low temperatures ($T < \theta/10$), the upper limit of the integration in equation (1) can be taken as infinity and equation (3) may be obtained:

$$\mathcal{G} = \text{constant} \times \frac{124.4T^5}{M\theta^6} \quad (3)$$

where the constant for each transition was calculated from Fig. 1, i.e., by employing $\frac{\Delta\rho}{\Delta T}$, θ the Debye temperature and M the atomic weight of chalcopyrite (CuFeS_2) i.e., 184 amu. Equation (3) was used for the Fig. 3. The plot of Grüneisen function in Fig. 3 is very interesting. It shows a sharp transition at 215 K, which is indicative of the fact that some kind of phonons, may be optical or acoustical, are excited at 215 K and become free from their respective Brillouin zones.

Figure 4 shows both theoretical and experimental results of thermoelectric power of chalcopyrite. The thermoelectric power undulations in chalcopyrite are increasing with increasing temperature. There is some kind of phase transition occurring at 240 K, where the maximum positive thermoelectric power is observed in the temperature range of 77-300 K. The theoretical thermoelectric power, S_{th} , is also calculated which shows a monotonic linear trend. The chalcopyrite sample, from Balochistan, has a room temperature thermopower value of 600 $\mu\text{V/K}$; as compared to -260

Table 1. The calculated values of activation energy, relaxation time, mean free path and Grüneisen function at all labelled transition temperature regions for chalcopyrite

Temperature T with labelled transition regions	$\frac{\Delta\rho}{\Delta T}$ $\times 10^{-4}$	Grüneisen function $\mathcal{G} =$ $\left(\frac{\Delta\rho}{\Delta T}\right) \frac{24.4T^5}{M\theta^6}$	Activation energy (from Arrhenius plot) with Boltzmann constant $k_B = 8.62 \times 10^{-5} \text{ eV/K}$	Activation energy (from Berry)	Temperature coefficient with $t_0 = 10^{-13} \text{ s}$ $\alpha = -\left(\frac{k_B}{Q_0}\right) \log\left(\frac{t_0}{t}\right)$	Relaxation time (from plot) with $t = 7.1 \times 10^{-4} \text{ s}$ $t_0 = \frac{t}{\exp\left(\frac{Q_0}{k_B T}\right)}$	Relaxation time (from Berry) $t = t_0' \exp\left(\frac{Q_0}{k_B T}\right)$	Mean free path with $v = v_0 = 3.41 \times 10^4 \text{ m/s}$ $l = vt_0$
(K)	($\Omega\text{-m/k}$)	(Arbitrary units)	(eV)	(K $^{-1}$)	(s)	(s)	(m)	(m)
92	E-F	3.1E-11	941.2	0.183824	0.000176	4.16E-14	0.00071	5.989E-09
183	D-E	-	-	-	-	0.00071	0.00071	102.24
209	C-D	2.93E-10	1599.7	0.35713	-0.0006	1.57E-11	0.00071	2.260E-06
215	B`-C	1.46E-09	8144.9	1.616914	0.001495	9.14E-42	0.00071	1.317E-36
221	B-B`	6.17E-10	5628.8	1.117421	0.001205	2.38E-29	0.00071	3.430E-24
300	A-B	1.13	108.73	0.021585	-0.03789	0.000308	0.00071	44.37334

Table 2. The calculated values of Debye temperature, Debye wave vector, Debye velocity, Fermi wave vector, Fermi velocity and Fermi energy for chalcopyrite

Sample	Debye wave vector with $\frac{N}{V} = 4.25 \times 10^{26} \text{ m}^{-3}$	Debye velocity with $\omega_D = 10^{14} \text{ rad/s}$	Debye temperature with $\hbar = 1.055 \times 10^{-34} \text{ Js}$ $k_B = 1.38 \times 10^{-23} \text{ J/K}$	Fermi wave vector with $\frac{N}{V} = 4.25 \times 10^{26} \text{ m}^{-3}$	Fermi velocity with $\hbar = 1.0552 \times 10^{-34} \text{ Js}$ $m = 9.11 \times 10^{-31} \text{ kg}$	Fermi energy $E_F = \frac{\hbar^2 k_F^2}{2m}$
	$k_D = \left(6\pi^2 \frac{N}{V}\right)^{1/3}$	$v_D = \frac{\omega_D}{k_D}$	$\Theta_{\text{theo}} = \left(\frac{\hbar v_D}{k_B}\right) \left(6\pi^2 \frac{N}{V}\right)^{1/3}$	$k_F = \left(3\pi^2 \frac{N}{V}\right)^{1/3}$	$v_F = \frac{\hbar k_F}{m}$	(eV)
Chalcopyrite (CuFeS ₂)	6.94×10^8	1.44×10^5	764.14	5.51×10^8	6.38×10^4	0.0115

and $-290 \mu\text{V/K}$; obtained by Kametani *et al.* (1990) from the chalcopyrite samples of Mount Isa mine and $120 \mu\text{V/K}$ by Izmailov and Silantev (1978). The higher value of thermoelectric power obtained might be due to pyrrhotite (Fe_{1-x}S ($x = 0$ to 0.2)), which plays a significant role in the conductivity of chalcopyrite as observed by Izmailov and Silantev (1978).

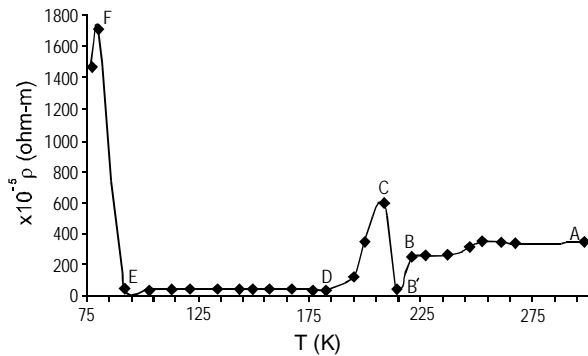


Fig. 1. Electrical resistivity vs temperature for chalcopyrite (CuFeS_2).

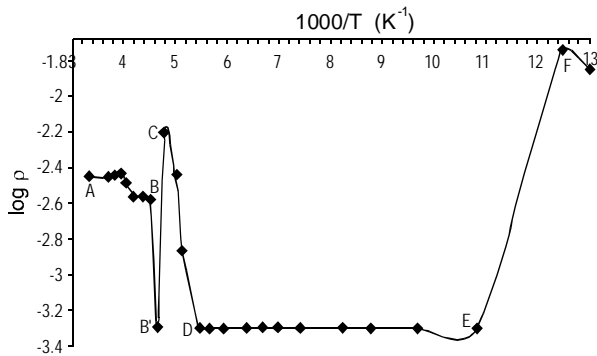


Fig. 2. Arrhenius plot for activation energies of chalcopyrite (CuFeS_2) i.e., $\log \rho$ vs $1000/T$.

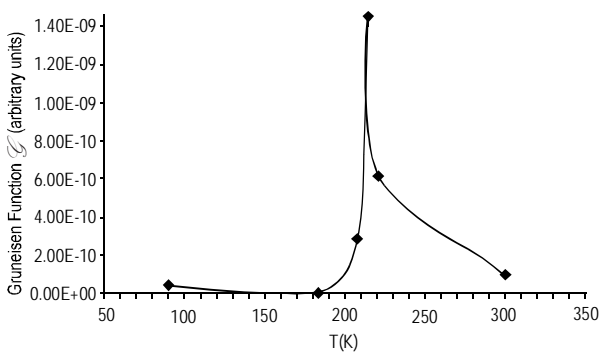


Fig. 3. Grüneisen function vs temperature for chalcopyrite (CuFeS_2).

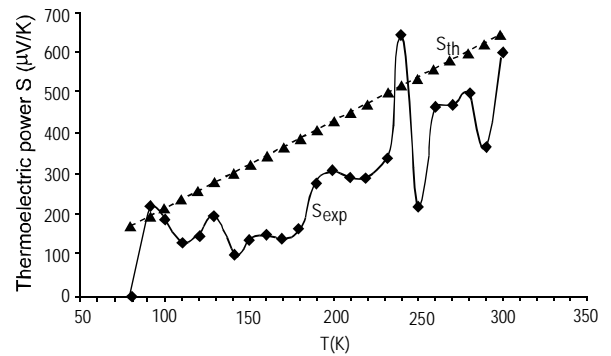


Fig. 4. Experimental and theoretical curves showing values of thermoelectric power (S) vs temperature for chalcopyrite (CuFeS_2).

There are many cases for estimating the theoretical thermoelectric power (Barnard, 1972), but we shall restrict to diffusion thermopower for a free electron metal or alloy obeying Fermi-Dirac statistics in which $E_F \gg k_B T$ (the degenerate case) and in which a single relaxation time exists. The theoretical thermoelectric power for a range of representative value of E_F is given by the following equation.

$$S_{th} = - \frac{\pi^2 k_B^2 T}{3|e|E_F} \quad (4)$$

where:

k_B = Boltzmann constant and
 e = charge of an electron.

Equation (4) is valid only if mean free path is regarded as a constant. The model of constant mean free path is applicable to electron scattering by impurity atoms and equation (4) is reduced to,

$$S_{th} = - \frac{2.45 \times 10^{-8} T}{E_F} \quad (5)$$

where:

E_F is in electron volts and
 T is in Kelvin.

Table 1 and 2 represent the calculated values and the formulae used for the parameters. The techniques used for such calculations, as mentioned in Table 1 and 2, are taken from the previous studies (Naqvi *et al.*, 1997; Raza *et al.*, 1995), excepting the Grüneisen function (Barnard, 1972; Rosenberg, 1963). Sulphur, being a constituent element of chalcopyrite, has two allotropes known as rhombic and monoclinic sulphur. Rhombic sulphur is energetically stable below 369 K. Hence, the sulphur in chalcopyrite exists in the form of rhombic

allotrope, in the temperature range, 78-300 K for electrical resistivity and thermoelectric power.

Conclusion

Summarizing the results, diverse transitions at various temperatures are observed in the study of electrical resistivity and thermoelectric power of chalcopyrite from room temperature down to liquid nitrogen temperature.

A semi-superconductivity transition in chalcopyrite is associated with formation of weak Fermions (not the Cooper pairs). A metal-insulator transition sets in at 92 K due to breakup of weak Fermions. Some kind of phonons, may be optic or acoustic, are excited at 215 K in chalcopyrite. Various semiconductor, imaging, nanotube, quantum well, optoelectronic and other devices based on this phenomenon can be designed using chalcopyrite (Steiner *et al.*, 2009; Ishii *et al.*, 2008, Kohara *et al.*, 2005; Vincent *et al.*, 2005, Lee *et al.*, 2003; Bai *et al.*, 2002). A phase transition due to diffusional recovery occurs at 240 K, indicated by the thermo-electric power study. A significantly high value of around 600 $\mu\text{V/K}$, room temperature thermopower was observed in the studied chalcopyrite sample.

Acknowledgement

Authors are thankful to the Higher Education Commission (HEC), for the award of grant to carry out research work and to the Dean Faculty of Science, University of Karachi, for financial support.

References

- Bai, X., Kurdak, C., Krishna, S., Bhattacharya, P. 2002. Quantum-well-based phonon detectors; performance analysis. *Physica B: Condensed Matter*, **316-317**: 362-365.
- Barnard, R.D. 1972. *Thermoelectricity in Metals and Alloys*, Taylor & Francis Ltd., London, UK.
- Donovan, B., Reichenbaum, G. 1958. Electrical properties of chalcopyrite. *British Journal of Applied Physics*, **9**: 474-477.
- Fujisawa, M., Suga, S., Mizokawa, T., Fujimori, A., Sato, K. 1994. Electronic structure of CuFeS_2 and $\text{CuAl}_{0.9}\text{Fe}_{0.1}\text{S}_2$ studied by electron and optical spectroscopies. *Physical Review B*, **49**: 7155-7164.
- Gibbs, G.V., Cox, D.F., Rosso, K.M., Ross, N.L., Downs, R.T., Spacman, M.A. 2007. Theoretical electron density distributions for Fe- and Cu-sulphide earth materials: a connection between bond length, bond critical point properties, local energy densities and bonded interactions. *Journal of Physical Chemistry B*, **111**: 1923-1931.
- Harris, M.J., Zankin, M.P., Swainson, I.P. 1997. Phonons and spin waves in the magnetic semiconductor chalcopyrites CuFeS_2 . *Physical Review B*, **55**: 6957-6959.
- Ishii, H., Kobayashi, N., Hirose, K. 2008. Effects of contacts to electrodes and phonon scattering on transport of carbon-nanotube devices. *Journal of Physics: Conference Series*, **100**: 052062, 1-4.
- Izmailov, L.I., Silant'ev, V.N. 1978. Thermoelectric properties of sulfides of a series of northeastern USSR deposit. *Mineral. i Geokhimiya Rudn. Mestorozhd. Sev.-Vost. SSSR, Magadan*, 81-87.
- Kametani, H., Kobayashi, M. 1990. Thermoelectric power measurements of particulate chalcopyrite samples from the Mount Isa Mine. *Aus IMM Proceedings*, **295**: 27-37.
- Kametani, H. 1982a. A novel method for thermoelectric power measurement of pulverized metal sulfide ores. *Nippon Kogyo Kaishi*, **98**: 47-52.
- Kametani, H. 1982b. Thermoelectric power of pulverized samples of chalcopyrite, white metal, copper matte and copper concentrates. *Nippon Kogyo Kaishi*, **98**: 119-124.
- Khabibullin, I.K., Schmidt, E.V., Matukhin, V.L. 2009. Study of electronic and magnetic properties of the CuFeS_2 semiconductor compound in the temperature range 77-300 K. *Semiconductors*, **43**: 1650-1653.
- Kohara, M., Megawa, S., Asakawa, M., Awazu, K., Tsubouchi, N. 2005. Recovery of silicon by coherent phonon excited by free electron laser irradiation. *Review of Laser Engineering*, **33**: 181-188.
- Kurmaev, E.Z., van Ek, J., Ederer, D.L., Zhou, L., Callcott, T.A., Perera, R.C.C., Cherkashenko, V.M., Shamin, S.N., Trofimova, V.A., Bartkowski, S., Neumann, M., Fujimori, A., Moloshag, V.P. 1998. Experimental and theoretical investigation of the electronic structure of transition metal sulphides: CuS , FeS_2 and FeCuS_2 . *Journal of Physics: Condensed Matter*, **10**: 1687-1697.
- Lee, I.H., Yee, K.J., Lee, K.G., Oh, E., Kim, D.S., Lim, Y.S. 2003. Coherent optical phonon mode oscillations in wurtzite ZnO excited by femtosecond pulses. *Journal of Applied Physics*, **93**: 4939-4941.
- Naqvi, S.M.M.R., Rizvi, S., Rizvi, S.D.H., Raza, S.M., Shams, N., Rizvi, Y. 2007. Electrical resistivity and thermoelectric power measurements of pyrite (FeS_2) in the temperature range, 78-300K. *Journal of The Chemical Society of Pakistan*, **29**: 549-552.
- Naqvi, S.M.M.R., Rizvi, S., Rizvi, S.D.H., Abbas, S.Z., Raza, S.M., Ahmad, M., Kamaluddin, S., Mahmood, Z. 2005. Magnetization behaviour of Pyrite (FeS_2) and Chalcopyrite (CuFeS_2) Minerals. In: *Proceedings of the 9th International Symposium on Advanced Materials*, pp. 429-433.

- Naqvi, S.M.M.R., Rizvi, S.D.H., Raza, S.M., Gormani, M.A., Rizvi, S. 1997. Study of nucleus size with iron contents in iron-zirconium LQA alloys at relatively high temperatures. *Solid State Communications*, **101**: 627-630.
- Naqvi, S.M.M.R., Rizvi, S.D.H., Jamila, S., Rizvi, S., Raza, S.M., Gormani, M.A., Farooqui, N. 1995a. Electrical resistivity of cobalt-boron alloys. *Modern Physics Letters B*, **9**: 1535-1538.
- Naqvi, S.M.M.R., Raza, S.M., Rizvi, S.D.H., Gormani, M.A., Farooqui, N. 1995b. Electrical resistivity of liquid-quenched amorphous alloys. *Modern Physics Letters B*, **9**: 195-200.
- Naqvi, S.M.M.R., Rizvi, S.D.H., Fatima, S., Raza S.M. 1993. Thermoelectric effects in Bi-Pb-Sr-Ca-Cu-O superconductor. *Modern Physics Letters B*, **7**: 1331-1334.
- Naqvi, S.M.M.R., Shams, N., Rizvi, S.D.H., Abbas, T., Raza, S.M., Zia ul Haq, S.M. 1991. Electrical resistivity and dynamic temperature X-ray diffraction of Co-B liquid quenched amorphous alloys. *Modern Physics Letters B*, **5**: 1883-1893.
- Nkoma, J.S., Ekosse, G. 1999. X-ray diffraction study of chalcopyrite CuFeS_2 , pentlandite $(\text{Fe, Ni})_9\text{S}_8$ and pyrrhotite Fe_{1-x}S obtained from Cu-Ni ore bodies. *Journal of Physics: Condensed Matter*, **11**: 121-128.
- Raza, S.M., Gormani, M.A., Farooqui, N., Ahmed, M.A., Abbas, T. 1995. On thermally activated electrical resistivity in metallic glasses. *Solid State Communication*, **95**: 329-333.
- Rosenberg, H.M. 1963. *Low Temperature Solid State Physics*, Oxford University Press, London, UK.
- Shay, J.L., Wernick, J.H. 1975. *Ternary Chalcopyrite Semiconductors, Growth, Electronic Properties and Applications*, Pergamon Press, New York, USA.
- Sirota, N.N., Zhalgasbekova, Zh.K., Sidorov, A.A. 1991. Root-mean-square displacements of ions and characteristic temperatures of chalcopyrite according to the X-ray diffraction data of 5-300 K. *Doklady Akademii Nauk SSSR*, **317**: 873-878.
- Sirota, N.N., Zhalgasbekova, Zh.K., Sidorov, A.A. 1989a. X-ray diffraction study of thermal expansion of chalcopyrite at 4-300 K, *Doklady Akademii Nauk SSSR*, **305**: 909-913.
- Sirota, N.N., Zhalgasbekova, Zh.K., Sidorov, A.A. 1989b. Intensity of Bragg reflections of chalcopyrite at 4-300 K. *Doklady Akademii Nauk SSSR*, **309**: 1104-1107.
- Steiner, M., Freitag, M., Perebeinos, V., Tsang, J.C., Small, P.J., Kinoshite, M., Yuan, D., Liu, J., Avouris, P. 2009. Phonon populations and electrical power dissipation in carbon nanotube transistors. *Nature Nanotechnology Letters*, **4**: 320-324.
- Teranishi, T. 1962. Magnetic and electric properties of chalcopyrite. *Journal of The Physical Society of Japan*, **17**: 263-267.
- Teranishi, T. 1961. Magnetic and electric properties of chalcopyrite. *Journal of The Physical Society of Japan*, **16**: 1881-1887.
- Vincent, B., Elmazria, O., LeBrizoual, L., Bouvot, L., Rouxel, D., Alnot, P., Kruger, J.K., Kollé, M. 2005. Microwave induced phonons imaging by Brillouin microscopy. In: *Proceedings of IEEE Ultrasonic Symposium*, pp. 1015-1018.